Spinodal Phase Separation in Liquid Films with Quenched Disorder

Manish Vashishtha,[†] Prabhat K. Jaiswal,[‡] Rajesh Khanna,[*,†] Sanjay Puri,[‡] and Ashutosh Sharma[¶]

Department of Chemical Engineering, Indian Institute of Technology Delhi, New Delhi, India, School of Physical Sciences, Jawaharlal Nehru University, New Delhi, India, and Department of Chemical Engineering, Indian Institute of Technology Kanpur, Kanpur, India

E-mail: rajkh@chemical.iitd.ac.in

Abstract

We study spinodal phase separation in unstable thin liquid films on chemically disordered substrates via simulations of the thin-film equation. The disorder is characterized by immobile patches of varying size and Hamaker constant. The effect of disorder is pronounced in the early stages (amplification of fluctuations), remains during the intermediate stages and vanishes in the late stages (domain growth). These findings are in contrast to the well-known effects of quenched disorder in usual phase-separation processes, viz., the early stages remain undisturbed and domain growth is slowed down in the asymptotic regime. We also address the inverse problem of estimating disorder by thin-film experiments.

[*]To whom correspondence should be addressed
[†]Department of Chemical Engineering, Indian Institute of Technology Delhi, New Delhi, India
[‡]School of Physical Sciences, Jawaharlal Nehru University, New Delhi, India
[¶]Department of Chemical Engineering, Indian Institute of Technology Kanpur, Kanpur, India

Introduction

Consider a system which is rendered thermodynamically unstable by a sudden change of parameters, e.g., temperature, pressure. The subsequent evolution of the system is characterized by the emergence and growth of domains enriched in the preferred phases.[1] This domain growth process is of great importance in science and technology. In this context, an important paradigm is the phase-separation kinetics of an initially homogeneous binary (AB) mixture. If the initial concentration fluctuations grow spontaneously, the evolution is referred to as *spinodal decomposition*. The segregating mixture evolves into coexisting domains of A-rich and B-rich phases. In pure (disorder-free) systems, these domains are characterized by an increasing length-scale, $L(t)$, which grows as a power-law, $L(t) \sim t^{\phi}$ in time t. The exponent ϕ depends on the transport mechanism. For diffusive transport, $L(t) \sim t^{1/3}$, which is known as the Lifshitz-Slyozov (LS) growth law and is based on the *evaporation-condensation* mechanism.[2]

In recent work,[3] we have emphasized the analogies and differences between usual phase-separation kinetics and the *spinodal phase separation* (SPS) dynamics of an unstable thin liquid film (< 100 nm) on a pure substrate. Typically, random fluctuations in the free surface of initially flat films grow and evolve into distinct morphological phases, viz., a thinner low-curvature flat film phase, and a thicker high-curvature droplet phase. Spinodal growth occurs when the excess intermolecular free energy $\Delta G(h)$ shows a minimum and the spinodal parameter, $\partial^2 \Delta G/\partial h^2|_{h=h_0} < 0$. Here, h is the film thickness, and h_0 is the average thickness.[4,5] In [figure][1][]1, we show a typical form of ΔG vs. h and the corresponding spinodal parameter, $\partial^2 \Delta G/\partial h^2$ vs h. The double-tangent construction for ΔG in [figure][1][]1 shows that the film segregates into phases with $h = h_m$ and $h = \infty$. (This should be compared with phase-separation problems, which are described by a double-well potential, and there are two possible values for the equilibrium composition.[1,6]) In an alternative scenario, commonly known as *true dewetting*, the thin film breaks up into dewetted dry spots (with $h = 0$) surrounded by undulating liquid ridges and there is no SPS.[4] Our recent work[3] on SPS on homogeneous substrates has shown that the number density of local maxima in the film's surface (defects), N_d, is a suitable marker to identify the early, late and intermediate stages

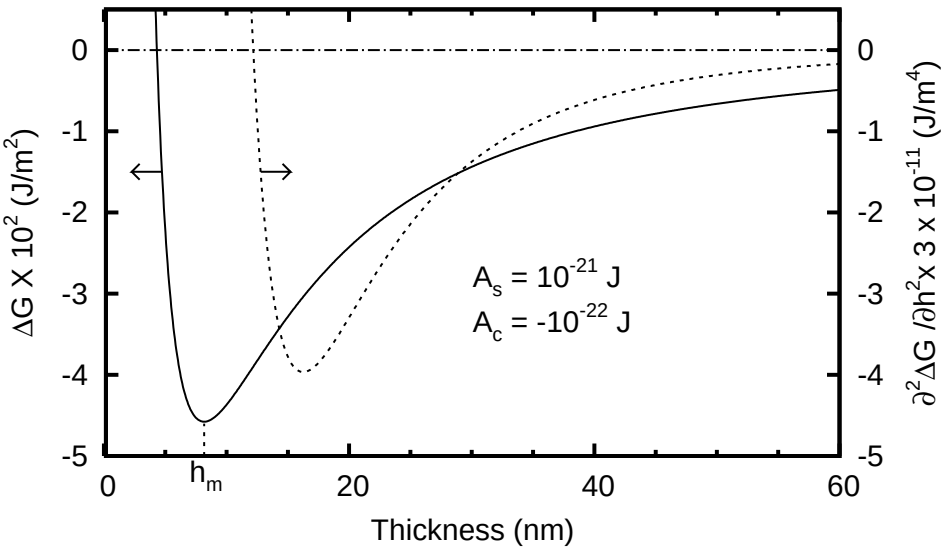

Figure 1: Variation of the free energy per unit area (ΔG, solid line) and spinodal parameter ($\partial^2 \Delta G/\partial h^2$, dashed line) with film thickness. The parameter values are $R = -0.1$ and $\delta = 10$ nm. Spinodal phase separation takes place for $h > 12.5$ nm, where $\partial^2 \Delta G/\partial h^2 < 0$.

of SPS in thin films. We have also established that the kinetics of the early stages can be described by a universal evolution of this marker with a suitably rescaled time, and the late stages can be described by the LS growth law.

The above discussion has focused on SPS in pure systems with homogeneous substrates. However, real experimental systems never satisfy this condition. The substrates contain physical and chemical impurities (disorder), which can be immobile (quenched) or mobile (annealed). We have some understanding of the alternative scenario of true dewetting on disordered substrates,[7] but the problem of SPS with disorder is yet to be addressed. This letter investigates SPS in unstable thin liquid films on substrates with quenched chemical disorder, and highlights novel features which arise due to the presence of disorder. The inverse problem of estimating the disorder through thin-film experiments is also addressed, as this would be very useful for experimentalists.

Model and Simulation

The starting point of our study is the thin-film equation which models the evolution of the film's surface $h(\vec{x},t)$ in supported thin liquid films. This is derived by simplifying the equations of motion via the *lubrication approximation*[8]. The resulting equation is analogous to the Cahn-Hilliard (CH) equation[9] of phase separation with an h-dependent mobility[10], $M(h) = h^3/(3\mu)$ (corresponding to Stokes flow with no slip). The total free energy is $F_s[h] = \int[\Delta G(h) + \gamma(\vec{\nabla}h)^2/2]d\vec{x} \equiv F_e + F_i$, where F_e is the overall excess free energy and F_i is the interfacial free energy. The quantities γ and μ refer to surface tension and viscosity of the liquid film, respectively. The corresponding CH equation is

$$\frac{\partial}{\partial t}h(\vec{x},t) = \vec{\nabla}\cdot\left[M\vec{\nabla}\left(\frac{\delta F_s}{\delta h}\right)\right] = \vec{\nabla}\cdot\left[\frac{h^3}{3\mu}\vec{\nabla}\left(\frac{\partial \Delta G}{\partial h} - \gamma\nabla^2 h\right)\right], \tag{1}$$

where all gradients are taken in the plane of the substrate. The potential $\Delta G(h)$ usually combines a long-range attraction and a short-range repulsion. The results presented here correspond to a long-range van der Waals attraction due to the substrate, and a comparatively short-range van der Waals repulsion provided by a nano-coating on the substrate:[11] $\Delta G = -A_c/12\pi h^2 - A_s/12\pi(h+\delta)^2$. This is the potential shown in [figure][1][]1. Here, A_s and A_c $(= RA_s)$ are the effective Hamaker constants for the system, which consists of the fluid above the film, the liquid film, and a solid substrate (s) or coating material (c). The thickness of the nano-coating is δ.

We can reformulate [equation][1][]1 in a dimensionless form as follows:

$$\frac{\partial}{\partial T}H(\vec{X},T) = \vec{\nabla}\cdot\left[H^3\vec{\nabla}\left(\frac{2\pi h_0^2}{|A_s|}\frac{\partial \Delta G}{\partial H} - \nabla^2 H\right)\right]. \tag{2}$$

In [equation][2][]2, $H = h/h_0$, where h_0 is the mean film thickness; $\vec{X} = \vec{x}/\xi$, where $\xi = (2\pi\gamma/\mid A_s \mid)^{1/2} h_0^2$ is the characteristic scale for the van der Waals case; and $T = t/\tau$, where $\tau = \left(12\pi^2\mu\gamma h_0^5/A_s^2\right)$. The excess free-energy term now has the form

$$\frac{2\pi h_0^2}{\mid A_s \mid}\frac{\partial \Delta G}{\partial H} = \frac{1}{3}\left[\frac{1-R}{(H+D)^3} + \frac{R}{H^3}\right], \tag{3}$$

where $D = \delta/h_0$ is the nondimensional coating thickness. The linear stability analysis of [equation][2][]2 for fluctuations about $H = 1$ predicts a dominant spinodal wave of wave-vector k_M and time-scale T_M with

$$k_M = \frac{2\pi}{L_M} = \sqrt{-\frac{\pi h_0^2}{|A_s|}\frac{\partial^2 \Delta G}{\partial H^2}\Big|_{H=1}} \equiv \sqrt{\frac{\alpha}{2}}\,,$$

$$T_M = \frac{4}{\alpha^2}. \tag{4}$$

For a homogeneous substrate, the parameters in [equation][2][]2-[equation][3][]3 are spatially uniform. We model the quenched disorder via fixed patches of varying size P with relative Hamaker constant R. The mean values of P and R are P_m and R_m. These parameters are uniformly distributed in the intervals $[P_m - \delta P, P_m + \delta P]$ and $[R_m - \delta R, R_m + \delta R]$, with $\delta P/P_m = P_d$ and $\delta R/R_m = R_d$. In [figure][2][]2, we plot the spinodal parameter $(2\pi h_0^2/\,|\,A_s\,|)\partial^2\Delta G/\partial H^2$ vs.

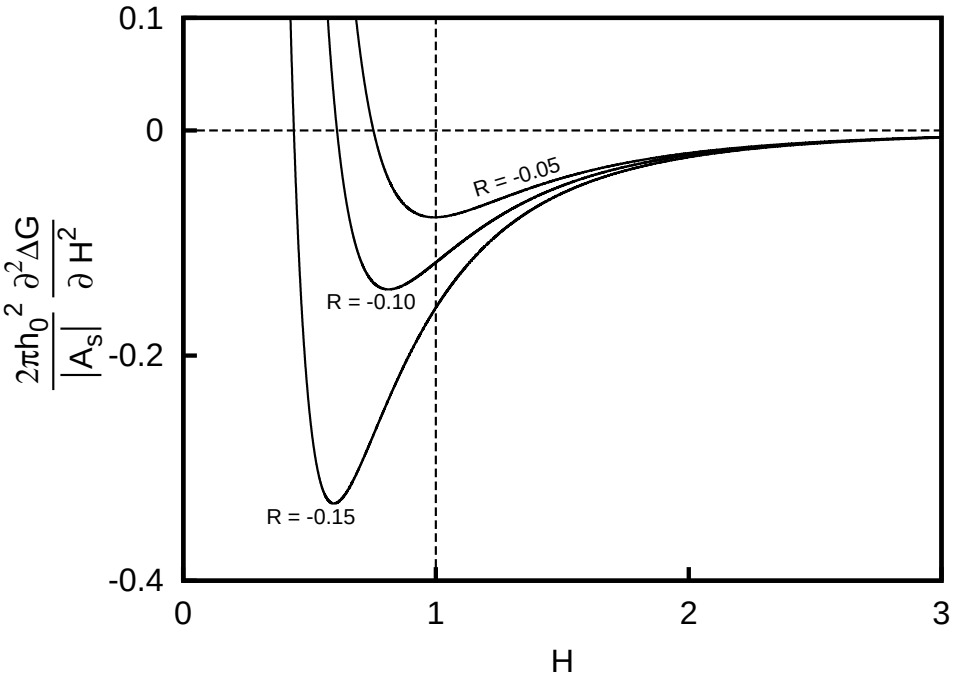

Figure 2: Variation of dimensionless spinodal parameter with nondimensional film thickness for three values of $R = -0.15, -0.1$ and -0.05.

H for three representative values of R. These correspond to the mean value $R_m = -0.1$, and the extreme deviations for $R_d = 0.5$. Notice that a small change in R results in a major change of k_M

(or L_M) and T_M in [equation][4][]4.

We numerically solve [equation][2][]2 in $d = 2,3$ starting with a small-amplitude ($\simeq 0.01$) random perturbation about the mean film thickness $H = 1$. The system size in $d = 2$ is $n\bar{L}_M$, where $\bar{L}_M$ is the dominant wavelength for $R = R_m$ (n ranges from 16 to several thousands). The system size in $d = 3$ is $(16\bar{L}_M)^2$. We apply periodic boundary conditions. A 512-point grid per $\bar{L}_M$ was found to be sufficient when central-differencing in space (with half-node interpolation) was combined with *Gear's algorithm* for time-marching, which is convenient for stiff equations. The parameters D, R_m and R_d were chosen so that the film is spinodally unstable at $H = 1$ (i.e., $\alpha > 0$) for all values of R. A typical spatial variation of R with $R_m = -0.1$ and $R_d = 0.5$ is shown in [figure][3][]3. P_m was taken as $f\bar{L}_M$, where f varies from 1/16 to 16. Thus, the size of the patches with fixed R varied from being much smaller than the spinodal length-scale to being much bigger than it.

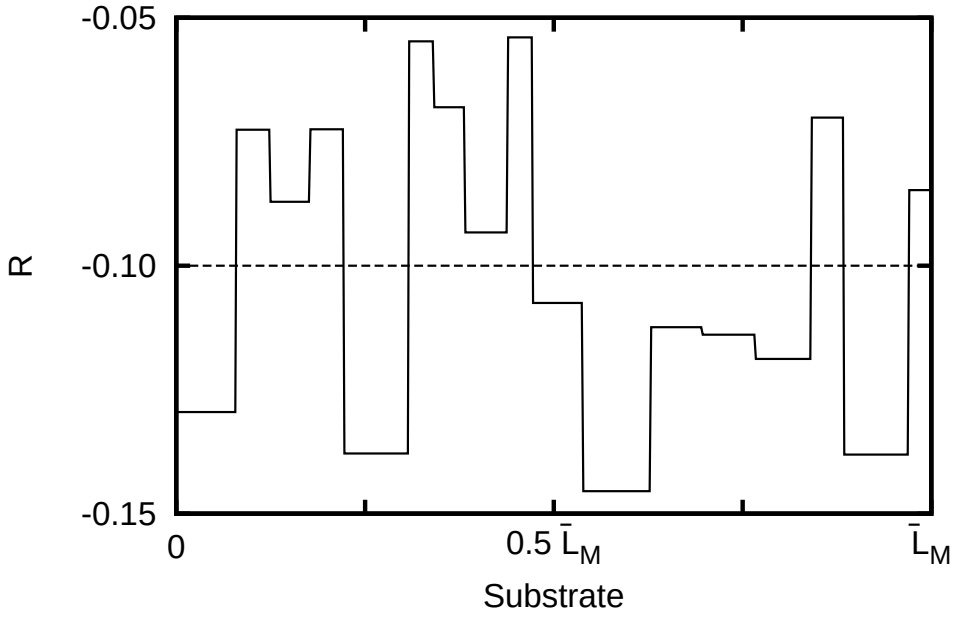

Figure 3: Schematic of a chemically disordered substrate. The disorder is quenched and is characterized by $R_m = -0.1$ (horizontal dashed line), $R_d = 0.5$, $P_m = \bar{L}_M/16$ and $P_d = 0.5$.

Results and Discussion

All the three markers of the process, viz., number density of defects (N_d), morphology and energy are affected by the strength (R_d) as well as the length-scale (P_m) of the chemical disorder. Notice that N_d^{-1} characterizes the typical domain size. In [figure][4][]4, we plot N_d vs. T on a log-log scale. The effect of disorder is pronounced in the early stages, persists during the intermediate stages, and vanishes in the late stages. The evolution of N_d briefly follows the results of the pure case ($R_d = 0$), but is seen to diverge while still in the early stages. However, surprisingly, the plot

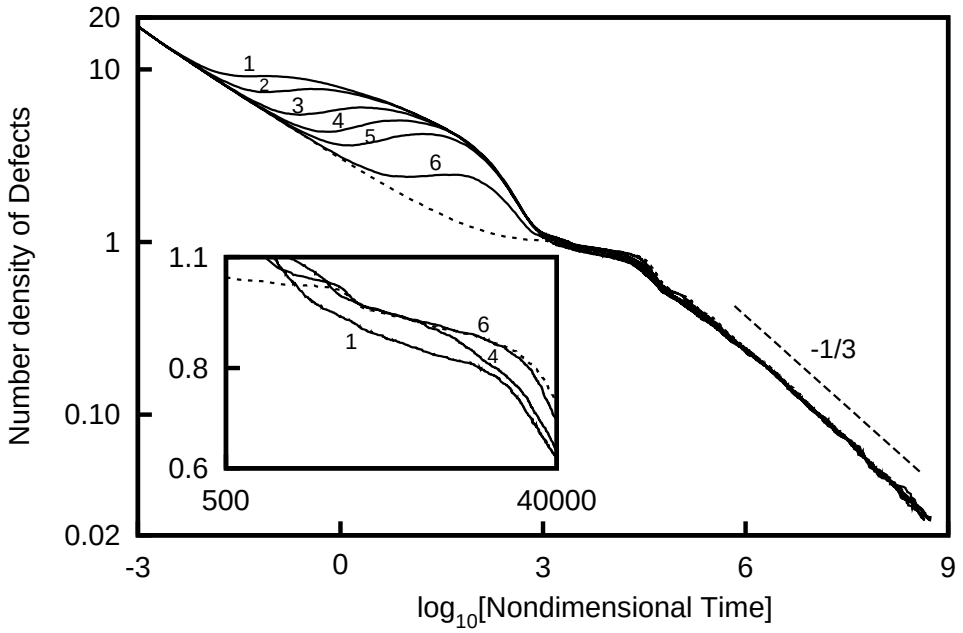

Figure 4: Variation of the number density of defects (N_d) with nondimensional time (T) for a $d = 2$ system of size 2048 $\bar{L}_M$ and $D = 0.5$. Curves 1 to 6 present results for $R_m = -0.1$ and $R_d = 0.50, 0.25, 0.10, 0.05, 0.03$ and 0.01, respectively. The LS $-1/3$ slope for late stages is shown by the dashed line. The dotted curve corresponds to the case with zero disorder (base case). The inset shows the magnified intermediate stage for $R_d = 0.50, 0.05$ and 0.01. The other parameter values are $P_m = \bar{L}_M/16$, $P_d = 0.5$.

of N_d vs. T reverts to the pure case in the late stages. This is the central result of this letter, and will be discussed shortly. The deviation in the intermediate stages is seen in the magnified view in [figure][4][]4. A decrease in the disorder strength delays the divergence, but even a weak disorder amplitude ($R_d = 0.01$) results in a sizable split (see [figure][4][]4). The split occurs because the

growth of initial fluctuations is drastically amplified by the presence of disorder ([figure][5][]5).

Consider the growth of initial fluctuations, $H = 1 + \theta(\vec{X}, T)$, in [equation][2][]2. On Fourier-transforming $\theta(\vec{X}, T)$ and integrating the resultant $\theta(\vec{k}, T)$ over a uniform disorder distribution on $[R_m(1-R_d), R_m(1+R_d)]$, we obtain

$$\bar{\theta}(\vec{k}, T) = \exp\left[k^2\left\{\alpha(R_m) - k^2\right\}T\right] \frac{\sinh(bk^2 R_m R_d T)}{bk^2 R_m R_d T}\, \theta(\vec{k}, 0), \tag{5}$$

where $b = 1 - (1+D)^{-4}$. The factor which represents the effect of the disorder, $\sinh(cT)/(cT)$, $\to 1$ as $R_d \to 0$, but amplifies the growth of initial fluctuations for nonzero R_d. In turn, this increases the sub-structure in the growing profile (see frames at $T = 0.052, 10$ in [figure][5][]5) – resulting in a slower decrease of N_d vs. T. The growing fluctuations are saturated in the late stages when domains are formed at the smaller value of the equilibrium thickness $H_m < 1$. Of course, the height field continues to grow for $H > 1$. These domains coarsen with time and obey the LS growth law.[3] The presence of disorder causes local fluctuations in the domain structure – see frame at $T = 10000$ in [figure][5][]5.

In the late stages, the growth law is universal in [figure][4][]4 ($N_d \sim T^{-1/3}$), regardless of the presence of disorder. This should be contrasted with the usual phase-separation problem, where coexisting domains are trapped by disordered sites.[12–14] The subsequent coarsening proceeds by thermally-activated barrier hopping, leading to an asymptotically logarithmic growth law. In the SPS problem discussed here, the defects consist of "interfaces" between flat domains at $H = H_m$ and growing hills with $H \to \infty$. These defects do not become trapped as the disorder scale becomes irrelevant in comparison to the diverging height of the "interfaces". This late-stage universality has important implications for experimentalists. As mentioned earlier, it is not possible to eliminate disorder from experimental systems. However, our results show that disorder is irrelevant in the late stages, and all experiments will finally recover results for the pure case. The differences between the pure and disordered systems only show up in the early stages, as quantified above.

The evolution of the total free energy is also consistent with the evolution of the defect density

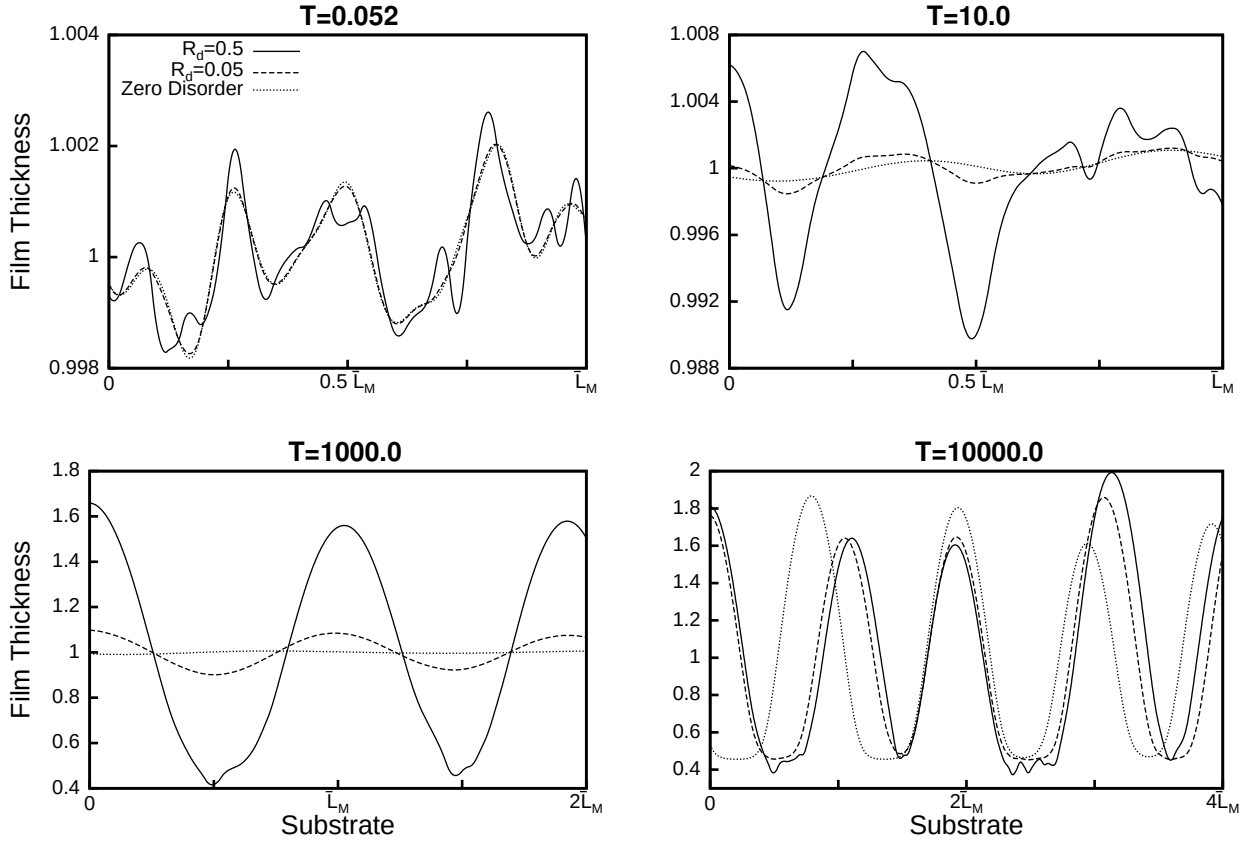

Figure 5: Morphological evolution of the film at different nondimensional times, as specified. We show results for $R = -0.1$ and $R_d = 0.5, 0.05$ and the pure case. The other parameter values are the same as in [figure][4][]4.

([figure][6][]6). As expected, the overall free energy diminishes with time. The decay in the late stages is a universal power-law, which is independent of the disorder amplitude. The difference between the pure and disordered cases is seen in the early stages, with faster decay for larger disorder values, as the growth of initial fluctuations is speeded up by disorder.

Next we focus on the effect of varying the patch size (P_m, P_d) on SPS. The early-stage kinetics exhibits three qualitatively distinct behaviors depending on the ratio f $(P_m = f\bar{L}_M)$. Notice that the limit $P_m \to$ system size corresponds to the pure case. For small values of f $(f < 1/2)$, the disorder leads to splitting as described earlier [Type A curves in [figure][7][]7(a)]. For intermediate values of f $(1/2 < f < 2)$, the disorder leads to a distinctive staircase behavior for N_d vs. T [Type B curves in [figure][7][]7(a)]. In this case, the patch size is comparable to the spinodal wavelength,

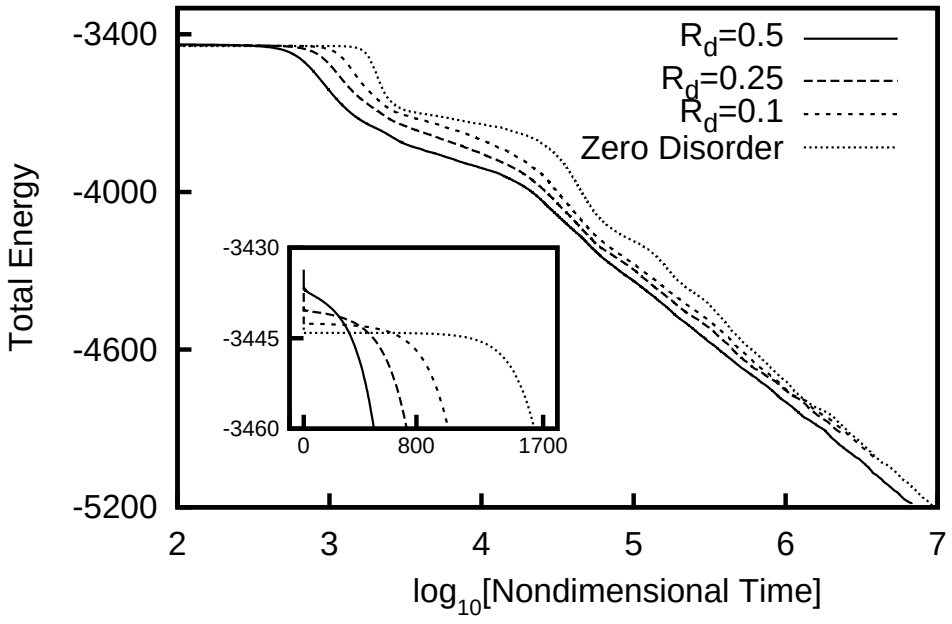

Figure 6: Variation of the total free energy with nondimensional time for a system of size 2048 $\bar{L}_M$ and $D = 0.5$. The curves present results for $R_m = -0.1$ and $R_d = 0.50, 0.25, 0.1$. The other parameter values are $P_m = \bar{L}_M/16$, $P_d = 0.5$. The dotted curve corresponds to the case with zero disorder. The inset shows the magnified view for energy variation in the early stages.

resulting in a stick-slip dynamics of the height field. For larger values of f ($f > 2$), the disorder has little effect and the early-stage kinetics resembles that for homogeneous substrates [Type C curves in [figure][7][]7(a)]. As expected, the late-stage dynamics is again universal with $N_d \sim T^{-1/3}$ – we do not show this regime in [figure][7][]7(a). A similar behavior is also seen in $d = 3$ simulations – in [figure][7][]7(b), we plot N_d vs. T for this case. The simulation details are provided in the figure caption.

As the spinodal length-scale can be controlled by changing the mean film thickness ($l_M \propto h_0^2$, where l_M is the dimensional length-scale), one can use the present findings to address the inverse problem of assessing the disorder by thin-film experiments. In thick films, we see Type A behavior because $f \ll 1$. A reduction in the film thickness such that $1/2 < f < 2$ results in Type B behavior. A further reduction in thickness ($f > 2$) results in Type C behavior. We can use Type C curves to first estimate L_M, and then R_m from [equation][4][]4. Thus, we can estimate the disorder amplitude to an order of magnitude. An average value found by monitoring the spinodal length-scale when

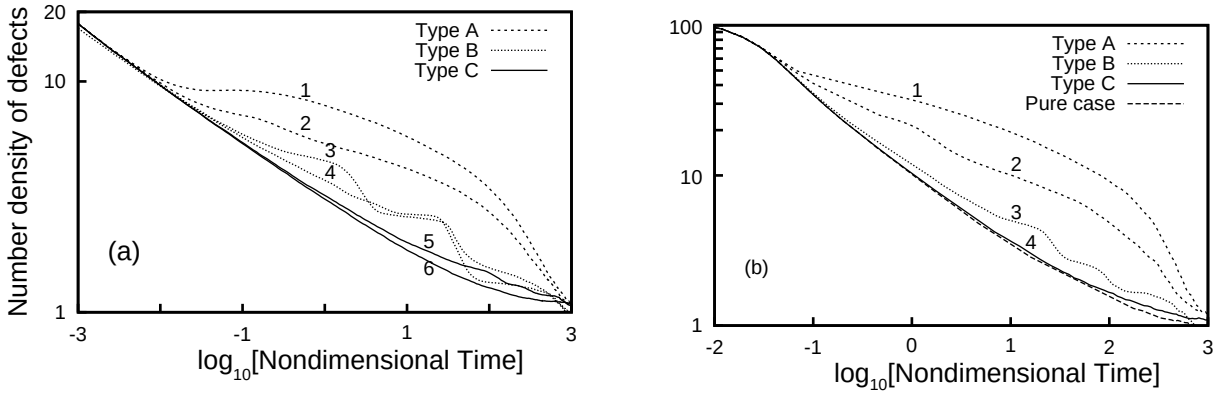

Figure 7: Variation of the number density of defects with nondimensional time in (a) $d = 2$ and (b) $d = 3$. The parameters are $R_m = -0.1$, $R_d = 0.5$. The different curves are obtained by varying the mean patch size $P_m = f\bar{L}_M$. We classify the curves as follows: Type A ($f < 1/2$), Type B ($1/2 < f < 2$), and Type C ($f > 2$).

Type B behavior starts and when it ends can fine-tune this estimate. The strength of the disorder can be found by any Type C result.

Conclusions

In summary, we conclude that quenched chemical disorder has a pronounced effect on the early and intermediate stages of morphological phase separation in thin liquid films. However, the late-stage kinetics is universal and follows the Lifshitz-Slyozov (LS) growth law. These findings are in sharp contrast to the effects of quenched disorder seen in usual phase-separation processes, viz., the early stages remain undisturbed and domain growth is slowed down in the asymptotic regime. The early-stage kinetics shows different qualitative behavior, depending on the relative sizes of disorder patches and the spinodal length-scale. Thus, the inverse problem of estimating disorder by thin-film experiments can also be addressed.

References

(1) *Kinetics of Phase Transitions*, 1st ed.; Puri, S., Wadhawan, V., Eds.; CRC Press: Boca Raton, Florida, 2009.

(2) Lifshitz, I. M.; Slyozov, V. V. *J. Phys. Chem. Solids* **1961**, *19*, 35–50.

(3) Khanna, R.; Agnihotri, N. K.; Vashishtha, M.; Sharma, A.; Jaiswal, P. K.; Puri, S. *arXiv:1001.2611* **2010**, *to be published*, .

(4) Sharma, A.; Jameel, A. T. *Journal of Colloid and Interface Science* **1993**, *161*, 190–208.

(5) Sharma, A.; Khanna, R. *Physical Review Letters* **1998**, *81*, 3463–3466.

(6) Bray, A. J. *Adv. Phys.* **1994**, *43*, 357.

(7) Kargupta, K.; Konnur, R.; Sharma, A. *Langmuir* **2000**, *16*, 10243–10253.

(8) Ruckenstein, E.; Jain, R. K. *Journal of Chemcal Society Faraday Transactions* **1974**, *70*, 132.

(9) Cahn, J. W.; Hilliard, J. E. *Journal of Chemical Physics* **1958**, *28*, 258.

(10) Mitlin, V. S. *Journal of Colloid and Interface Science* **1993**, *156*, 491.

(11) Khanna, R.; Jameel, A. T.; Sharma, A. *Industrial and Engineering Chemistry Research* **1996**, *35*, 3081–3092.

(12) Puri, S.; N.Parekh, *Journal of Physics A* **1992**, *25*, 4127.

(13) Paul, R.; Puri, S.; Reiger, H. *Europhysics Letters* **2004**, *68*, 881.

(14) Paul, R.; Puri, S.; Reiger, H. *Physical Review E* **2005**, *71*, 061109.